AD-A284 279

AR-008-154

DEPARTMENT OF DEFENCE

DSTO

Optoelectronics Division

DTIC
ELECTE
SEP 09 199

S
B

D

SURVEILLANCE RESEARCH LABORATORY

RESEARCH NOTE
SRL-0114-RN

**TESTING AND CHARACTERISATION OF THE 'CYCLOPS'
HgCdTe FOCAL PLANE DETECTOR ARRAY**

by

G. V. Poropat

94-29561

DTIC QUALITY INSPECTED 3

APPROVED FOR PUBLIC RELEASE

AR-006-154

DSTO♠
A U S T R A L I A

SURVEILLANCE RESEARCH LABORATORY

Optoelectronics Division

RESEARCH NOTE
SRL-0114-RN

TESTING AND CHARACTERISATION OF THE 'CYCLOPS' HgCdTe FOCAL PLANE DETECTOR ARRAY

by

G.V. Poropat

SUMMARY

Optoelectronics Division has developed an advanced technology demonstrator utilising an infrared focal plane detector array to assess the feasibility of using passive infrared sensors for ADF applications. To model the performance of the sensor the characteristics of the focal plane detector array have been measured. The measurement of the characteristics of large scale detector arrays and the testing of these arrays present problems which are not encountered with single element infrared detectors. Optoelectronics Division has gained considerable experience in these processes during the development of the 'Cyclops' technology demonstrator. The procedures used in characterising the HgCdTe focal plane detector array and the results obtained are described.

AUG 93

DTIC QUALITY INSPECTED 3

APPROVED FOR PUBLIC RELEASE

CONTENTS

FIGURES

APPENDICES

1 INTRODUCTION

Optoelectronics Division of the Surveillance Research Laboratory (SRL) has developed an experimental infrared sensor system that utilises a large scale infrared focal plane detector array (FPDA). The sensor system operates in the long-wave infrared (LWIR) spectral region and has been called 'Cyclops'. The detector array consists of photodiodes fabricated on a mercury cadmium telluride (HgCdTe, MCT or CMT) wafer with readout electronics fabricated on a silicon wafer to which the detector array is physically bonded and electrically connected. The technology demonstrator has been used to test the capabilities of infrared systems utilising FPDAs for ADF applications.

A mathematical model of the 'Cyclops' sensor system has been developed to analyse the performance of the system and predict signal to noise ratios for a variety of targets and operating conditions [1]. The operation of the model requires detailed knowledge of sensor characteristics such as the spectral response and noise performance and properties of the target and the operating environment. The measurement of the required detector characteristics is described in this paper.

Some earlier (smaller) arrays of HgCdTe detectors were constructed so as to permit access to individual detectors. However the architecture of the array used in the 'Cyclops' system does not allow direct connection to the individual elements of the array. The measurement of the characteristics of the detectors which comprise the FPDA therefore cannot be done using the techniques that are used for testing conventional, ie single element, detectors [2].

Particular difficulties are encountered in the measurement of the electrical bandwidth and the noise power spectral density of the detectors in a FPDA. The construction of the detector array requires the acquisition of data on the noise performance of the detectors in a form which differs from that obtained for conventional detectors. This paper describes the procedures used to undertake measurements of the detector array used in the 'Cyclops' system and describes the results obtained. The measurements described here are of importance since such measurements will be required for the development, testing and maintenance of future FPDA based systems.

2 THE 'Cyclops' SENSOR SYSTEM

The focal plane detector array which provides the imaging capability of the 'Cyclops' sensor system consists of 16,384 individual detectors arranged as 128 rows of 128 detectors. The detectors are fabricated on a HgCdTe wafer with a centre to centre spacing between the detectors of 20 μm. The detectors are photodiodes with a photon spectral response of approximately 5.5 μm to 10.5 μm where the upper and lower limits of the spectral response are defined by the 50% response points of the normalised spectral responsivity.

The cutoff wavelength of the long wave spectral response of the detectors is determined by the band gap of the $Hg_{1-x}Cd_xTe$ semiconductor from which they are fabricated. The bandgap is dependent on the Hg concentration in the alloy [3, 4, 5] which is specified by the x value in the composition of the alloy. Due to the difficulty of manufacturing HgCdTe wafers with a uniform Hg concentration there is a considerable variation in the long wave cutoff of the spectral response of the photodiodes in a large array of detectors. This variation contributes to non uniformity in the responsivity of the detectors which comprise the array.

The detector array is made by Philips Infrared Components using a proprietary process, referred to by the manufacturer as 'loopholing'. The process uses a metal connection laid over the HgCdTe wafer through a hole machined in the wafer to achieve the connection between the photodiode and the multiplexer / readout circuitry which is fabricated on the silicon substrate [6]. The sensitive area of the detector is thus an annulus centred on the hole through which the contact to the substrate is made. This structure is illustrated in Figure 1. The manufacturing process differs significantly from the technique based on the use of indium bump bonding which is used by some other manufacturers [7, 8]. The array is read out using an electronically scanned interface circuit and is known as a MESA [6, 9] (multiplexed electronically scanned array). A simplified schematic of the detector array and focal plane readout circuitry is presented in Figure 2.

In a photodiode, photons which are energetic enough, ie have wavelengths shorter than the long wave cutoff, generate pairs of carriers which are separated by the diode field. In the staring mode

a detector views a constant segment of the object space and a common mode of operation of FPDAs involves integration of the carriers generated in the detectors for a defined time, the 'stare time'. The integrated charge is then read out as the detector signal.

In the 'Cyclops' array, the storage capacitors used to accumulate the carriers generated in the detectors are fabricated on the silicon substrate. The limited charge storage capacity which can be provided on the focal plane has resulted in an array architecture with one set of 128 capacitors for storage of the carriers generated in the detectors.

To use the integrating capacitors, one line of detectors is electrically connected to the integrating capacitors and for the stare time, each detector continuously images an instantaneous field of view determined by the size of the detector and the focal length of the optical system used. The array thus operates in a line scanned equivalent mode. The electronically scanned multiplexer allows the array to be operated in this mode without the requirement for mechanical scanning. Each column of photodiodes is connected to the 128 storage capacitors via a set of FET gates as shown in Figure 2. The charge accumulated on each capacitor during the stare time is then read out and presented at the output of the multiplexer as a series of voltages. These voltages are amplified by electronic circuitry off the focal plane and then converted to digital signals using a 16 bit analogue to digital converter.

At the end of the stare time the integrating capacitors are reset and then electrically connected to the next column of detectors to integrate the carriers generated in them during the next stare time. The duty cycle of each detector in the array is therefore determined by the number of columns of detectors in the array (128). When allowance is made for the time taken to read the signals, the pixel stare time is approximately 0.0075 of the frame time. For this FPDA the pixel stare time is usually 200 μseconds to 300 μseconds. Since the scanning is performed electronically, the detectors are not required to respond to time varying signals as they would have to in a mechanically scanned imager unless there are temporal changes in the scene distribution which have a rate of change which is significant when compared to the stare time.

The readout circuit includes a dynamic shift register and the use of this circuit component with the charge store and read mode of operation prevents direct or 'permanent' connection to any individual photodiode in the detector array. This limitation prevents the user from performing some of the measurements normally used to characterise infrared detectors. The development of focal plane detector arrays has therefore required new techniques for measuring their characteristics and methods of specifying their performance characteristics [2].

The charge transfer efficiency of the integration, multiplexing and readout circuitry for this detector array is not specified by the manufacturer. Neither the charge transfer efficiency of the integrating and readout circuits nor the quantum efficiency of the detectors can be measured using the equipment available within Optoelectronics Division. The charge transfer efficiency has therefore been inferred from other measurements. Analysis of the physics of the operation of the array and the mathematical formulation of the sensor response are relatively insensitive to minor errors in the measurement of this parameter.

For this array, the most significant limitation on performance is the variation of the responsivities of the detectors from element to element in the array. This variation is in part dependent on the variation of the cutoff wavelength of the responsivity of each detector. The variation in the responsivity of the detectors in the array is the primary effect which determines the noise equivalent temperature difference (NETD) of the array. Due to the large scene temperature ranges expected, the internal noise of the detectors in the array and the readout noise do not affect the NETD to the same extent as the nonuniformity of the responsivities of the detectors. The nonuniformity in responsivities essentially determines the overall performance of the array when imaging an extended source ie a source with an extent such that the resolution limits imposed by the optical system and the detector spacing do not affect the detector output signal.

3 DETECTOR RESPONSIVITY

The spectral responsivity of an infrared detector is the ratio of the rms signal voltage (or current) to the rms value of the monochromatic incident signal power, referred to an infinite load impedance and to the terminals of the detector [3]. The blackbody responsivity of an infrared

detector is defined similarly [3] and is the ratio of the rms signal voltage (or current) to the rms value of the incident signal power arising from a blackbody source. These definitions are not strictly applicable to the elements of a focal plane detector array since the detectors are interfaced to the device terminals by multiplexing and buffering circuits but they can be used without modification if the definitions are taken to refer to the responsivity of the detector array and the on-chip electronics as a composite device.

For detector arrays and single element detectors, responsivity can be measured as the black body responsivity or 'overall' responsivity (sometimes called 'in band' responsivity) or the spectrally dependent responsivity can be measured [2]. The choice of which responsivity is used will determine the procedures required for the measurement of the responsivity and influence the analysis of sensor operation based on the results of the measurements.

When characterising single infrared detectors or FPDAs where direct access to the detector is possible, the response to a chopped source of infrared radiation is measured since this technique allows the attainment of much greater signal to noise ratios. The MESA readout from the detectors in the array used here produces a series of voltage pulses as the array output. The form of this output signal prevents the use of narrow band electronic filters tuned to the chopping frequency, therefore, the improvement in signal to noise ratio which is normally afforded by the use of a chopped radiation source cannot be achieved for measurement of the responsivity of the elements of this detector array.

Aside from the problem of chopping the source radiation at the frequencies that the image frames are acquired (typically from 10 Hz to 100 Hz), synchronisation is required to ensure that the array is uniformly illuminated during the stare time in each frame. This synchronisation may be difficult to achieve for staring arrays. Synchronisation of the source of infrared radiation would enable measurements of responsivity to be undertaken which can be corrected to remove any low frequency drift in the response of the system but this is a relatively unimportant requirement.

The results of measurements of responsivity provided by the manufacturer of the detector array are in the form of specifications of the detector current observed when the array is illuminated with a blackbody source. These data are thus 'in band' responsivities. To be able to effectively model the performance of the detector array we have measured the spectral variation of the detector responsivity for selected elements of the array and related this to the 'in band' responsivity through the use of the mathematical model of the detector performance.

The observed responsivity of the elements of the array is dependent on the charge transfer efficiency and the detector quantum efficiency. Estimates of these have been obtained for the array used by comparing the measured increment in the observed output voltage for a change in source temperature to the calculated increment in the observed output voltage for the same change in source temperature. The number of carriers generated due to the irradiance from an extended source at short range (atmospheric transmission effects are therefore negligible) on the elements of the detector array is

$$
n_p = \tau . \upsilon . \Omega . \eta_{peak} . A_c \int_{\lambda_0}^{\lambda_{co}} \eta(\lambda). L_{q,\lambda}(\lambda, T). \tau_{lens}(\lambda) d\lambda \tag{1}
$$

where $\eta(\lambda)$ is the normalised detector spectral quantum efficiency and $L_{q,\lambda}$ is the spectral photon sterance (radiance) of the source. The emission from the source is obtained using Planck's law which gives the spectral distribution of the photon emission per steradian per unit wavelength interval, $L_{q,\lambda}$, from a black body at temperature T [3]. In this equation, $\tau_{lens}(\lambda)$ is the spectral transmission of the lens, η_{peak} is the peak detector quantum efficiency and λ_0 and λ_{co} are the wavelength limits of the spectral response of the sensor.

Using measured data for the spectral response of an element of the detector array and the lens used with the array, the increment in the observed output voltage for a change in source

temperature is compared to the calculated response for an element of the array. The detector and system characteristics are detailed in Appendix 1. The relevant data required here are:

integration time (τ)	300 μseconds
detector fill factor (ν)	0.377
optical aperture collecting area (A_c)	0.00288 metres^2
detector site instantaneous field of view (Ω)	$1.6 \cdot 10^{-7}$ steradian

where the detector IFOV is defined by the area of the detector site ($4.0 \cdot 10^{-10}$ metres^2) and the focal length of the lens (50 mm).

Using source temperatures of ice (273.16K), 20.1°C and 30.5°C the ratio of the measured output voltage increments observed when the detector array was illuminated with sources at these temperatures was 0.586. Using the equation above and the same source temperatures with an emissivity of 0.95 for ice and 0.99 for the other calibration source, the ratio of the increment in the predicted output voltages is 0.592. The correlation between these results indicates that the measured spectral responsivity of the detector (including window) and the spectral response of the lens are accurate measures of the spectral response of the system.

The system used to acquire data from the FPDA uses a preamplifier to buffer the output signals from the detector array. The preamplifier has a voltage gain of 2 and the output signal from the preamplifier is digitised using a 16 bit analog to digital converter. The capacitance used for charge storage for each photodiode on the focal plane is 2.2 picofarad. Although no detailed data has been made available by the manufacturer of the detector array, the peak spectral quantum efficiency of the photodiodes comprising the detector array is specified as typically 0.7. Using this data, laboratory measurements indicate that the charge transfer efficiency from the photodiodes to the array output is of the order of 0.75.

With this value of charge transfer efficiency, an output signal of 1 volt requires the accumulation of $1.373 \cdot 10^7$ electrons on the storage capacitance. An accumulated charge of 698 electrons on the storage capacitance will then increment the analog to digital converter output by one count.

The broad band responsivity obtained from these measurements is approximately $1.05 \cdot 10^8$ Volts/watt for blackbody illumination in the 7 μm to 12 μm spectral region. The responsivity is dependent on the integration time used. It can be seen that for these measurements, the specification of broad band responsivity in Volts/watt provides little more than an indicator of the range of signal levels which might be observed when using the detector array and is meaningless in terms of detailed performance analysis.

In summary, the detector characteristics are:

detector peak quantum efficiency	0.7
detector cold shield F/#	0.826
detector fill factor (ν)	0.377
integration capacitance	2.2 picofarad
charge transfer efficiency	0.75
preamplifier voltage gain	2
integration time	300 μseconds
carrier count per bit	698

4 SPECTRAL RESPONSE OF THE DETECTOR ARRAY ELEMENTS

The spectral response of the detectors is an important characteristic of sensor since the response of the elements of the detector array varies with the wavelength of the incident radiation. The variation of the response with wavelength is a complex function of the physics of the operation of the array and the construction of the array. Conceptually, the measurement of the spectral response of the elements of the detector array is straight forward; the measurement is performed using essentially similar equipment to that used for single element detectors and as the wavelength of the incident radiation is varied, the detector output is measured and the variation with spectral content thus determined.

The variation of the responsivity of the detectors with wavelength is treated by using a normalised spectral quantum efficiency derived from the measured response of these detectors. The spectral quantum efficiency is then scaled by the peak quantum efficiency of the detector which is specified by the manufacturer as being typically 0.7.

Since the architecture of the 'Cyclops' array prevents the used of the standard technique of illuminating the detector with chopped radiation and using narrow band signal processing to obtain good a signal to noise ratio, measurements of individual pixel voltages were made. The variation of detector response with wavelength was obtained using a standard monochromator to select the wavelength of the radiation illuminating the detector array. A high temperature black body was used as the source of infrared radiation. A pyroelectric detector with uniform broad band spectral response was used as a reference detector to calibrate the system so that variations in the transmission of the measurement system across the spectral band of interest could be accounted for.

The measurements of spectral responsivity were performed by acquiring frames of data as the spectral content of the illuminating radiation was varied. The detector output voltages were digitised by the processing electronics and the 'image' frame data stored on magnetic media. The variation of the detector output with the spectral content of the illuminating radiation is then readily determined. The spectral response as measured includes the response of the transmitting window which is used to seal the dewar housing, the detector and any antireflection coating applied to the array. A plot of the spectral response of 'typical' detector is shown in Figure 3 with the theoretical cutoff defined by the Fermi distribution of carriers. The spectral transmission of the lens used in the sensor system is also shown for comparison.

5 LINEARITY OF RESPONSIVITY

The linearity of the responsivity of a detector is determined by observing the output signal over a linear range of values of the irradiance on the detector. This is, in effect, a measurement of the incremental responsivity of the detector. For this detector parameter to have meaning the irradiance on the detector must be determined in terms of the number of photons incident on the detector in the spectral band to which the detector exhibits useful response.

Other effects such as the linearity of the signal conditioning electronics, the linearity and monotonicity of the analogue to digital and digital to analogue converters used and the effect of any processing undertaken to correct the detector response can affect linearity of response. These effects must be taken into account if a complete measure of the detector linearity is to be undertaken.

The measurements described here, which have been used to determine the effective charge transfer efficiency and the peak quantum efficiency provide a measure of the linearity of the detector and the supporting electronics. The observed response of the detectors shows no quantifiable effects which have been attributed to nonlinearity in response and no further measurements have been undertaken to determine the linearity of response of the detectors in the array.

6 RESPONSIVITY NONUNIFORMITY

A major limitation on the performance of the HgCdTe FPDA based sensor developed by Optoelectronics Division is the nonuniformity of the responsivities of the detectors comprising the array. For systems utilising staring focal plane detector arrays (FPDAs), the nonuniformity of the responsivities of the elements of the array creates 'fixed pattern' noise which reduces the target to background signal to noise ratio. The amplitude of the fixed pattern noise remaining after processing is applied to correct for the nonuniformity in responsivities is dependent on the correction algorithm which is used to compensate for the nonuniformity [10].

The nonuniformity in responsivities is corrected by measuring the response of individual photodiodes when imaging blackbody sources at a set of known temperatures and using this data to perform two or three point correction on the responsivity of each diode [10].

The fixed pattern noise observed with this array is not static. The detectors are effectively direct coupled and the $^1/_f$ noise of the detectors is thus observed as a component of the output signal. $^1/_f$ noise processes are non-stationary and evolve with time, ie the mean and standard deviation are not constant. Therefore, the output signal of a detector imaging a constant source increases or decreases with time due to $^1/_f$ noise and this change will appear as an apparent change in the responsivity of individual detectors. The time evolution of the fixed pattern noise is dependent on the evolution of the $^1/_f$ noise of the detector elements and associated electronics and has components which are uncorrelated from detector to detector. For single detectors, $^1/_f$ noise is usually eliminated by implementing a low frequency cutoff in the temporal response of any processing electronics but this cannot be done for the array described here.

The effect of this on the performance of an imaging system is a time dependent degradation of target to background signal to noise ratio. The $^1/_f$ noise of each of the detectors is not correlated, therefore the variation of the detector output signals due to $^1/_f$ noise will change the apparent responsivities of the detectors randomly. This change in the apparent distribution of responsivities will reduce the probability of the detection of features within an image. In practice, the effect of the evolution of the $^1/_f$ noise processes is accommodated by recalibrating the array regularly.

The detector array was calibrated in the laboratory by making a series of measurements of the detector outputs when imaging a uniform source. The residual spatial noise remaining after the compensation algorithms were applied, was determined from these measurements. Averaging the image data over a series of frames acquired in a time period short enough so that the effects of the evolution of $^1/_f$ noise can be ignored was used to reduce the contribution from temporal noise sources and produce a more accurate determination of the true spatial noise.

The FPDA sensor system includes a real time processor which performs correction for detector responsivity non-uniformity. The residual non-uniformity is expressed in terms of a root mean square (rms) variation of the apparent temperature observed when imaging a uniform extended source. This rms variation can be expressed as an equivalent rms flux variation, and thus a rms variation in the number of carriers generated, which can then be added in quadrature to the photon noise and the system noise. The equivalent mean square variation in carriers (sec^{-2}) due to spatial noise when imaging a uniform extended source is

$$n^2{}_{fpn} = (\frac{A_d . \pi}{4.F^2})^2 \frac{\sum_{all\_pixels} (\int_{\lambda_o}^{\lambda_{co}} \eta(\lambda).(L_{q,\lambda}(\lambda,T_{pixel}) - L_q(\lambda,T_{average})).\tau_O(\lambda)d\lambda)^2}{no\_pixels} \qquad (2)$$

where T_{pixel} is the apparent temperature producing the observed pixel output, $T_{average}$ is the image average temperature and no_pixels is the number of pixels in the image, in this case the number of detectors in the array. Using $T_{average}+\delta T$ instead of T_{pixel} allows calculation of n_{fpn} from a knowledge of the residual detector responsivity nonuniformity when this is expressed as a rms image temperature variation. The number of noise electrons per pixel is then given by

$$N_e = \sqrt{t_s . n_b + n_{fpn}{}^2 + (\frac{t_s . i_n}{e})^2} \qquad (3)$$

where t_s is the pixel integration time. For the detector array used, a detector responsivity nonuniformity producing a rms image temperature variation of 0.1 K is equivalent to a rms carrier variation of $1.8 \cdot 10^8$ carriers per second. This approach provides a convenient method of including in the overall noise the spatial noise generated by residual nonuniformities in the responsivity of the detectors in the array after compensation has been applied for such nonuniformities.

The standard deviation of the image data for a number of image frames was obtained when viewing a uniform source. The average standard deviation of the digital image data observed was 165 cou:.. This corresponds to a rms scene temperature variation of 0.35 K. This is. effectively. the s" 'em NETD. However. a number of significant points in relation to this quantity must be noted.

The NETD as determined here is a measure of fixed pattern noise and will affect the ability of an observer to extract information from an image in a manner which is different to the effect of temporal noise. The conventional derivation of minimum resolvable temperature difference (MRTD) cannot be undertaken using this data.

The NETD measured here is greater than the NETD specified for many infrared imaging systems. however the sensitivity of this system is very high. The NETD is dependent on the scene temperature range which the system. and thus compensation algorithms. are expected to display. The 'Cyclops' system can accommodate scene temperature ranges of up to 60 K and for these applications an NETD of 0.35 K is representative of a very high performance infrared imaging system. For many systems. scene temperature ranges of 5 K to 10 K are the norm and NETDs of much better than 0.1 K can be achieved but these NETDs cannot be maintained for large scene temperature ranges. Restricted scene temperature ranges of 5 K to 10 K are not applicable to much of the Australian environment.

7 TEMPORAL NOISE

The treatment of noise in the analysis of conventional imaging systems cannot be readily applied to detector arrays which are operated in the mode described here ie where the detector signal is integrated for a fixed period. For scanning systems where the detector is the first stage in a signal processing chain which is continuous in time the detector can be considered as acting as a low pass filter. The scanning process exposes the detector to a time varying irradiance and the output of the detector is a complex. continuous. time varying function of the image content. the sensor optics. the scanning rate and the temporal response of the detector. Standard techniques of signal analysis utilising the bandwidth and the noise power spectral density (psd) of the detector are then used in the measurement of the detector characteristics and prediction of the sensor performance.

The detector noise current psd can be calculated from the short circuit photocurrent and the zero bias resistance[11] as

$$i_n^2 = \frac{4kT}{R_o} + 2qI_D.[amp^2 / Hz]$$ (4)

or. if a $^1/_f$ noise component is included. as[12]

$$i_n^2 = \frac{4kT}{R_o} + 2qI_D + \frac{cI_D^2}{f}.[amp^2 / Hz]$$ (5)

where c is a constant which is dependent on the particular detector. Typical measurements performed by DRA Malvern on early two dimensional arrays of 32 by 32 HgCdTe detectors have shown average R_oA products of the order of 10 Ωcm^2. with R_o values of the order of 10^4 Ω and short circuit photocurrents of the order of 200 nanoamps. These values result in a detector noise psd of $50.0 \cdot 10^{-26} amp^2 Hz^{-1}$ ($42.0 \cdot 10^{-26}$ $amp^2 Hz^{-1}$ plus $6.4 \cdot 10^{-26}$ $amp^2 Hz^{-1}$). For a detector bandwidth of 1 MHz such devices would exhibit noise currents of 70.0 picoamperes.

Carriers are continuously produced by thermal generation and by the absorption of incident background radiation. The charge collected in the storage capacitance then consists of a number of components: charge due to integration of the thermal (or dark) current. charge generated by the absorption of the background irradiance and charge generated by the absorption of irradiance from the object space of the sensor. The dark current itself consists of a number of components including a component due to carrier generation-recombination and diffusion of carriers from the substrate.

Noise analysis based on the use of noise psd is often not practically realisable for FPDAs. The analysis of detector signal to noise ratio using the detector noise psd is difficult to apply when the charge generated by the absorption of photons from the source is accumulated for a defined period and then transferred to the sensor electronics by some means of charge transfer which is effectively a discrete event. In addition, measurement of the noise psd cannot be made directly. For systems using staring arrays which integrate the carriers generated in each detector, it is convenient to model the total system noise as an equivalent noise generator in parallel with the detector. The pixel noise can be conveniently modelled with this equivalent detector noise current which is integrated for the stare time.

Since it is not possible to measure the noise psd of the elements of a focal plane detector array the availability of data on noise psd depends on whether the manufacture of the array makes such measurements during construction of the array or is prepared to provide data obtained during development of the array. Manufacturers often quote the number of noise electrons counted per pixel and it is possible to make measurements which provide an estimate of the effective number of noise carriers as seen at the output of the detector array. For users of detector arrays, such measurements can provide enough data to enable the prediction of the performance of a sensor using the detector array.

With the simplification that the detectors in the array view a s   e which does not vary in radiance during the stare time, which for this detector array is typi   200 μseconds to 300 μ seconds, the major temporal noise sources are photon noise and 'front end' system noise including the inherent noise of the detector. The front end system noise is contributed to by the noise from the readout and conditioning circuits which process the detector output. This description of the noise processes in the detector array does not include spatial noise which arises from other causes and is manifested in a different manner.

When a wide band white noise process is integrated for a defined time period, T, the variance of the integrated process can be determined from the autocorrelation function of the noise process [12]. Referring to Appendix 1, if the process being integrated is a noise current with a 'white' psd of a^2 amps²Hz⁻¹, and the integration is performed for period T, the variance of the integrated process is

$$\sigma_S^2 = \frac{Ta^2}{2\pi} \qquad (6)$$

If the noise signal is a current with psd of a^2amps²Hz⁻¹ the integrated signal is a charge (in coulombs) and the variance of the integrated signal has the units of coulombs².

For the detector array used, the R_0 values are of the order of $5.0 \cdot 10^6$ Ω and we have assumed that the manufacturers have achieved a lower short circuit photocurrent, say 100 nanoamps. These values result in a detector noise psd of $3.3 \cdot 10^{-26}$amp²Hz⁻¹ ($8.0 \cdot 10^{-28}$ amp²Hz⁻¹ plus $3.2 \cdot 10^{-26}$ amp²Hz⁻¹). For a wide band noise power current density of $3.3 \cdot 10^{-26}$ amp²Hz⁻¹ integrated for 300 μseconds, the variance in the collected charge due to the noise current will be approximately $10.0 \cdot 10^{-30}$ coulomb² and the standard deviation will therefore be $3.0 \cdot 10^{-15}$ coulomb or approximately $1.9 \cdot 10^4$ electrons.

The data provided with the detector array by the manufacturer indicates that the effective wide band detector noise current is approximately 10 picoamperes. Laboratory measurements made after delivery indicated a slightly higher equivalent wide band noise current of approximately 12 picoamperes; these measurements were made at the outputs of the dewar and used support electronics developed by OED. The sensitivity of these measurements can be gained from the fact that attachment of probes during the measurements, resulted in an average standard deviation of the pixel voltages observed at the output of the array of 11.0 millivolts corresponding to an equivalent detector noise current of 55 picoamperes; the majority of the observed noise in this case was induced external to the detector.

Measurements of the system noise were undertaken using the system used in the field experiments. This system uses a preamplifier with a voltage gain of 2 to buffer the detector signals

before analogue to digital conversion is performed. The noise was measured by recording the detector data for a set of photodiodes and using the previous results in terms of charge transfer efficiency etc to estimate the equivalent wide band detector noise current for the whole system.

Using this method, for the system used in the experimental trials, the average equivalent wide band detector noise current, which includes all system noise, is 21 picoamperes. Converting this to a form where it is expressed in terms of an equivalent electron count, the equivalent pixel electron count is approximately $3.9 \cdot 10^4$ electrons for an integration time of 300 μseconds. The noise performance of the sensor system used in the experimental trials is therefore approximately half as good as the performance which could ideally be achieved for the detector array used.

8 EVOLUTION OF SPATIAL NOISE WITH TIME

The observed sensor noise is a combination of the residual nonuniformities of the responsivity of the detectors in the array, temporal noise arising from the detector, the readout and interface electronics and photon noise as well as $^1/_f$ noise. For infrared imaging systems using single detectors which are mechanically · anned over object space, the signal conditioning circuits usually impose a low frequency cutoff which eliminates the effect of $^1/_f$ noise.

As has been described previously, $^1/_f$ noise is a non-stationary process which evolves with time: ie for $^1/_f$ noise the mean and standard deviation of the process are not constant with time. The effect of this can be observable drift in the output of each detector if there is no low frequency cutoff in the frequency spectrum of the temporal response of the detector and associated electronics. For the FPDA used in the 'Cyclops' sensor there is, effectively, no low frequency cutoff in the signal conditioning circuit.

The spatial noise which remains in the image of a uniform source distribution produced by an IRFPDA after nonuniformity correction has been applied is therefore not a stationary process. In practice, the drift is overcome by implementing a one point recalibration. The additive constant used in the nonuniformity compensation is adjusted using the data from each detector obtained when imaging a constant source and the effects of long term drift are eliminated.

This process requires the ability to provide a uniform source of stable temperature during operation and is therefore difficult to implement. The frequency with which the one point calibration must be applied is dependent on the method of uniformity compensation used, the $^1/_f$ noise present and the level of residual spatial noise which can be tolerated. An analysis of this is beyond the scope of this report.

9 COMPENSATION FOR VARIATIONS IN DETECTOR RESPONSIVITY

In practice, the FPDA is operated with a real time processor which corrects for the variation in detector responsivity from element to element in the array. For imaging scenes in normal operation this processor scales the image data after correction to accommodate a predetermined scene temperature range. The scene temperature range used is 253 K to 313 K which was selected due to the nature of the application for which the sensor has been designed. In this application, monotonic scene brightness response was required for lines of sight which would encompass terrestrial features and sky backgrounds.

In operation, the nonuniformity correction processor is transparent to the user apart from the requirement to calibrate the sensor when the sensor is first operated. Unless the sensor is operated for long periods or in an environment where the ambient conditions change recalibration is not usually required. However for the modelling of the response of the sensor and the analysis of performance of the sensor, the operation of the processor must be well calibrated.

The compensation for responsivity non-uniformity generally used for imaging is a two point linear compensation scheme. For imaging when maximum sensitivity is required a nonlinear three point compensation scheme which is capable of producing much lower residual spatial noise than the two point compensation scheme is used [10]. When the two point compensation scheme is used, an offset (individually determined for each pixel) is subtracted from the pixel data for each pixel and the pixel data is then scaled by multiplying the pixel data value with a predetermined scaling coefficient. The pixel data is acquired as 16 bit data and the output data is 16 bit data.

The compensation scheme is implemented using a linear model for the sensor response to blackbody scene temperature and requires two parameters for each pixel, the offset and the scaling coefficient. These parameters are calculated from the pixel data obtained when imaging a blackbody source at two known temperatures. When calibrating the array, the temperatures of the two calibration sources are entered and these temperatures are used to determine the calibration coefficients so as to produce the specified scene temperature range of -20° C to $+40^\circ$ C.

For the two point compensation scheme, the sensor response is modelled as being of the form

$$V = a.T + c \tag{7}$$

where V is the detector output voltage when imaging a scene of blackbody temperature T. The compensation scheme is then implemented so that for a scene temperature of T_{min} (253 K) the normalised video data output is zero and for a scene temperature of T_{max} the normalised video data output is one. The video data output is then scaled by 65536 to produce a 16 bit digital output. To achieve this an offset is subtracted from the detector output where

$$offset = a.T_{min} + c \tag{8}$$

and the data is then scaled with a scaling coefficient

$$scale = \frac{1}{a.(T_{max} - T_{min})} \tag{9}$$

so that the normalised output voltage is

$$V_{out} = \left(\frac{V_{in}}{65536} - offset\right).scale.65536 \tag{10}$$

where the detector parameters a and c are calculated from the image data obtained when imaging the calibration sources. The parameters a and c are given by

$$a = \frac{V_2 - V_1}{T_2 - T_1} \tag{11}$$

and

$$c = V_2 - T_2.a \tag{12}$$

where V_1 and V_2 are the detector output voltages observed when imaging blackbody sources at temperatures T_1 and T_2.

The linear model of detector response to scene temperature used in this compensation scheme is not an accurate representation of the response of the sensor to scene temperature since the photon flux emitted by a blackbody at temperature T varies as T^3. The effect of the limited spectral response of the detectors is to produce an apparent response to scene temperature of the form of T^b where b is approximately 5 and varies with the spectral response of the detector. The nonuniformity of the spectral responses of the elements of the detector array can be a major contributor to the overall nonuniformity of the responsivity of the detectors in the array and is the reason that the three point compensation scheme produces much lower residual spatial noise [10]. Three point compensation may be difficult to implement due to the difficulty of maintaining three blackbody sources and in field trials two point compensation may have to be used.

The sensor has been designed to display data, when suitably calibrated, with apparent zero range blackbody temperatures over the range 253 K to 313 K. The calibration data can be acquired using two black body sources with temperatures within this range. In practice, since the temperature data is entered manually, the calibration temperatures may be specified as being other

than the actual temperatures used if it is required that the display accommodate data outside the nominated range or if the available calibration sources do not lie within the temperature range 253 K to 313 K. The operation of the compensation processor is unaffected by this but the apparent scene temperature will change if the specified calibration temperatures change.

The measurement of apparent scene temperature differences based on signal differentials in image data must account for the effects of the calibration and compensation processes if the temperature estimates to be obtained are required with any degree of accuracy. The effect of the calibration temperatures on scene data is shown in Figure 4 where the compensated data resulting from sources with apparent black body temperatures of 253 K to 313 K obtained using three sets of calibration sources is displayed. Minor differences in the processor output data are observed when calibration temperatures of 30° C and 39° C are used with a calibration temperature of 0° C. A marked offset in the output data is produced when a calibration temperature of -50° C is used with a calibration temperature of 0° C.

The variation with apparent scene temperature of the calculated sensor output data, ie uncompensated scene data, for a typical photodiode observed for a range of apparent scene temperature increments is shown in figure 5. From this data is can be readily seen that the determination of apparent scene temperature increments is highly dependent on the apparent background scene temperature. The major effect which can be observed is that the increment in scene data for a given increment in scene temperature increases nonlinearly with the apparent background temperature. This effect is consistent with the physics of the situation but the band limited spectral response of the sensor results in a complex temperature dependency which cannot be adequately approximated by the T^3 variation with temperature of total photon emission from a black body.

In the trials conducted, calibration sources at 223 K and 273 K were used and the calibration temperatures used as input for the compensation processor were 255 K and 305 K. The calibration source temperatures were used because the observed scene temperature range extended below 253 K and 'dry ice' was the only stable temperature reference available during the conduct of the experiments. The apparent black body temperature of the 'dry ice' was measured using an Omegascope hand held radiometer with an assumed source emissivity of unity. The apparent calibration source temperatures as observed by the 'Cyclops' sensor will differ from this temperature due to the differing spectral responses of the radiometer and the 'Cyclops' sensor however the differences affect only the scaling of the output data.

Figure 6 shows the calculated compensation processor output data for the 'Cyclops' sensor using calibration sources at 223 K and 273 K sources and calibration temperature settings of 255 K and 305 K for the compensation processor. In practice, since the output of the nonuniformity compensation processor is 16 bit digital data, output data values in excess of 65535 'wrap around' when the least significant bit is lost and are displayed as black pixels.

10 FIGURES OF MERIT

The detector figure of merit, D*, has not been referred to here. The use of D*, which embodies concepts of signal bandwidth and noise psd in the estimation of the performance of infrared systems, is common practice in the analysis of scanned infrared sensor systems. This is an approach which is inherently difficult to apply to a 'staring' detector array since the development of D* is based on continuous time processes more suited to scanned detectors with continuous readout. The problems in the use of D* with detector arrays arise principally from the use of a restricted signal bandwidth in the measurement process and the use of a chopped source of radiation. Signal bandwidth has no meaning in the conventional sense with respect to staring detector arrays which integrate the charge carriers produced in the detector for a fixed time and transfer the charge to an output circuit. The difficulties associated with the use of a chopped source of radiation for measurements with detector arrays have been discussed previously.

An assumption which has been made in the measurements undertaken is that the temporal variation in the image flux distribution is negligibly small during the measurement period. This assumption removes the necessity to consider the detector as an element in a linear continuous time signal processing system. This approach allows a treatment of the noise processes observed

with the 'Cyclops' sensor to be used which is more closely related to measurable quantities such as the number of noise electrons per pixel.

A figure of merit has been developed for the specification of infrared detector arrays which appears to be suitable for certain applications of these arrays [2]. It has the form

$$D_a^* = \frac{SB^{0.5}}{N(P/A)A_D^{0.5}}$$

where S is the response to a 500 K blackbody which illuminates the detector array uniformly with a power density P/A Wcm^{-2}, N is the standard deviation of successive readings of an individual pixel, B is half the pixel rate and A_D is the area of the focal plane divided by the number of detectors.

The figure of merit has not been used here or in the prediction of the performance of the technology demonstrator which has been developed because it does not provide an approach to such predictions which makes accessible an estimate of performance for the applications considered. The use of the sensor with scenes which have very few (if any) features with apparent (or real) temperatures in excess of approximately 313 K means that the figure of merit D_a^* must be translated to this lower temperature to account for the markedly different spectral distribution of the detector irradiance at 313 K and 500 K. In addition, the figure of merit is specified in energy units and the pixel rate does not relate directly to the detector stare time. The latter may not be common to all arrays but the nature of the interface electronics used in this system means that there is not a linear relationship between pixel rate and stare time.

A major drawback to this figure of merit for our applications is imposed by the lack of a useful means of embodying the nonuniformity of the responsivity of the detectors in the array. For the detector array used the major limitation on performance is the nonuniformity of the responsivity of the detector elements and the figure of merit does not directly address this aspect of the performance of the array. Including the effect of responsivity nonuniformity in the term N in the definition of D_a^* does not allow us to account for the operation of the nonuniformity correction processor.

11 SUMMARY

The physical characteristics of the focal plane detector array are determined by the design and manufacturing processes and are detailed in the relevant data provided by the manufacturer. These data are summarised in Appendix 1 with additional relevant data for the sensor system.

Operating characteristics of the detector array which have been measured or inferred from measurements are summarised here.

Detector peak spectral quantum efficiency	0.7
Array charge transfer efficiency	0.75
Equivalent detector noise current (laboratory system)	0.4 picoamp·√Hz^{-1}
Equivalent detector noise current (Cyclops system)	0.9 picoamp·√Hz^{-1}
Preamplifier voltage gain	2
Integration time	300 μseconds
Carrier count per bit (with a preamp gain of 2)	698

The analysis of the data obtained using the 'Cyclops' sensor in field trials has been based on the results obtained in the laboratory testing described here. Two important corrections must be made in the use of field data. The first of these is the correction for the reduction in the focal plane irradiance from a source at long range due to the effects of atmospheric transmission. This is accomplished through the use of the program LOWTRAN to calculate the atmospheric emission and transmission for the experimental conditions and the use standard procedures to incorporate this data in the analysis.

A less obvious correction arises from the need to account for the effect of optical blurring on the observed signature of sources which have a spatial extent which is less than the detector IFOV.

This can be accounted for with the use of a suitable model of the optical blurring [15]. The requirement to correct for optical blurring is demonstrated by the fact that, if blurring is ignored, the calculated detector signal for the array used will be 18 per cent greater than the observed signa for a square source and 35 per cent greater than the observed signal for a circular source when the source images have an extent on the focal plane of 20 μm.

12 CONCLUSION

The testing and characterisation of large scale arrays of infrared detectors is a difficult and time consuming process. Australian laboratories do not, as yet, have a well developed capability to undertake these measurements and it will be essential that such a capability is developed if Australia is to be able to provide testing and service facilities for infrared imaging systems which use large scale detector arrays when they are introduced into service.

The testing of the functionality of large scale focal plane detector arrays requires complex electronic support to operate the arrays and extract and process the detector signals. The characterisation of these arrays is even more complex since characterisation requires a significant measurement capability in excess of that required to establish the functionality of such devices.

The procedures described here have been used to test the operation of a large scale focal plane detector array of 16384 LWIR HgCdTe photodiodes. The results obtained are in good agreement with the manufacturers data and have been used in the modelling of the operation of the array.

REFERENCES

1   G.V. Poropat, 'Sensor Modelling For The 'Cyclops' Focal Plane Detector Array Based Technology Demonstrator", SRL-0112-RN , 1992

2   R.G. Humphreys, 'Specification of infrared detectors and arrays', Infrared Physics, Vol 28 No 1, 1988, p29-35

3   W.L. Wolfe, G.J. Zissis (editors), 'The Infrared Handbook', Office of Naval Research, Washington DC, 1985

4   G.L. Hansen, J.L. Schmit, T.N. Casselman, 'Energy gap versus alloy composition and temperature in $Hg_{1-x}Cd_xTe$', Journal of Applied Physics, Vol 53, p7099, 1982

5   E. Sand, Y. Nemirovsky, 'Calibration curve for the cut-off wavelength of photodiodes in $Hg_{1-x}Cd_xTe$ epilayers', Infrared Physics, Vol 25 No 3, 1985, p591-594

6   M.A. Keenan, I.M. Baker, J.E. Parsons, R.A. Ballingall, P.N.J. Dennis, T.W. Ridler, 'Advances in linear and two dimensional HgCdTe-Si hybrid focal plane arrays', IEEE Int. Conf. on Advanced Infrared Detectors and Systems, Pubn 204, p54 (1981)

7   J.P. Rode, 'HgCdTe hybrid focal plane', Infrared Physics, Vol 24 No 5, 1984, p443-453

8   R. Balcerak, J.F. Gibson, W.A. Gutierrez, J.H. Pollard, 'Evolution of a new semiconductor product: mercury cadmium telluride focal plane arrays', Optical Engineering, March 1987, Vol 26 No 3 p191-200

9   I.M. Baker, J.E. Parsons, R.A. Ballingall, I.D. Blenkinsop, 'Two dimensional infrared focal plane arrays utilising a direct inject input scheme', SPIE Proceedings, Vol 685, "Infrared Technology XII" (1986)

10 G.V. Poropat, 'Nonlinear compensation for responsivity nonuniformities in cadmium mercury telluride focal plane detector arrays for use in the $8\mu m$ to $12\mu m$ spectral region', Optical Engineering, Vol 28 No 8 p887-896, August 1989

11 I.M. Baker, M.D. Jenner, R. Lockett, R.A. Ballingall, I.D. Blenkinsop, D.J. Lees 'Two dimensional random access infrared arrays', IEEE Int. Conference, Pubn 228, p6 (1983)

12 N. Bluzer, A.S. Jensen, 'Current readout of infrared detectors', Optical Engineering, March 1987, Vol 26 No 3 p241-248

13 A.M. Papoulis, 'Probability, random variables and stochastic processes', McGraw Hill, New York 19

14 A.M. Papoulis, 'Systems and transform with applications in optics', McGraw Hill, New York 1968

15 G.V. Poropat, 'The effect of system point spread function, apparent size and detector instantaneous field of view on the infrared image contrast of small objects', Optical Engineering, (accepted for publication) 1993.

or the detector array and focal plane readout circuitry is presented in Figure 2.

In a photodiode, photons which are energetic enough, ie have wavelengths shorter than the long wave cutoff, generate pairs of carriers which are separated by the diode field. In the staring mode

UNCLASSIFIED   I

APPENDIX 1: MESA Focal Plane Detector Array and System Characteristics

Philips Components Multiplexed Electronically Scanned Detector Array E2908/5 Characteristics

Detector pitch	$20\,\mu m$
Detector outer radius	$8\,\mu m$
Detector inner radius	$4\,\mu m$
Detector area fill factor	0.377
Detector cold shield F/#	0.826
Integration capacitance	2.2 picofarad

'Cyclops' System Characteristics

Lens focal length	50 mm
Lens F/#	0.8
Optical aperture area	0.00288 metres^2
Lens blur spot: α	$2.932*10^{10}$ metres^{-2}

APPENDIX 2: Integration of noise processes

Given a real valued stochastic process, x(t), we want to determine the mean and variance of the signal obtained by integrating the process over a finite time interval. a,b. Designate the output of the integrator as S. then

$$S = \int_a^b x(t)dt \qquad (1)$$

The mean of S is

$$E\{S\} = E\left\{\int_a^b x(t)dt\right\} \qquad (2)$$

$$= \int_a^b E\{x(t)\}dt$$

which for a zero mean process is identically zero. For a zero mean process, x(t), the variance of S is

$$\sigma_S^2 = \int_a^b \int_a^b E\{x(t_1)x(t_2)\}dt_1dt_2 \qquad (3)$$

which is

$$\sigma_S^2 = \int_a^b \int_a^b C(t_1,t_2)dt_1dt_2 \qquad (4)$$

where $C(t_1,t_2)$ is the autocovariance function of x(t) [13]. For a stationary process

$$\sigma_S^2 = \int_{-2T}^{2T} (2T - |\tau|).C(\tau)d\tau \qquad (5)$$

or if $C(\tau)$ is even then

$$\sigma_S^2 = 2\int_0^{2T} (2T - |\tau|).C(\tau)d\tau \qquad (6)$$

where the integration time, previously a to b, is now 2T (-T to +T)[13].

If we consider x(t) as a wide band white noise process with power per unit bandwidth (power spectral density) of a^2Volts^{2}Hz^{-1}, the autocorrelation function of this process is $a^2\delta(t)(2\pi)^{-1}$. Then using equation 5

$$\sigma_S^2 = \int_{-2T}^{2T} (2T - |\tau|).\frac{a^2\delta(\tau)}{2\pi}d\tau \qquad (7)$$

$$\sigma_S^2 = \frac{Ta^2}{\pi} \qquad (8)$$

Redefine the period of integration from -T to +T (an interval of 2T) to an interval of $-T/_2$ to $+T/_2$, an interval of T. The variance of the signal obtained by integrating $x(t)$ over time T is $Ta^2(2\pi)^{-1}$ with units of Volts^2 s^2.

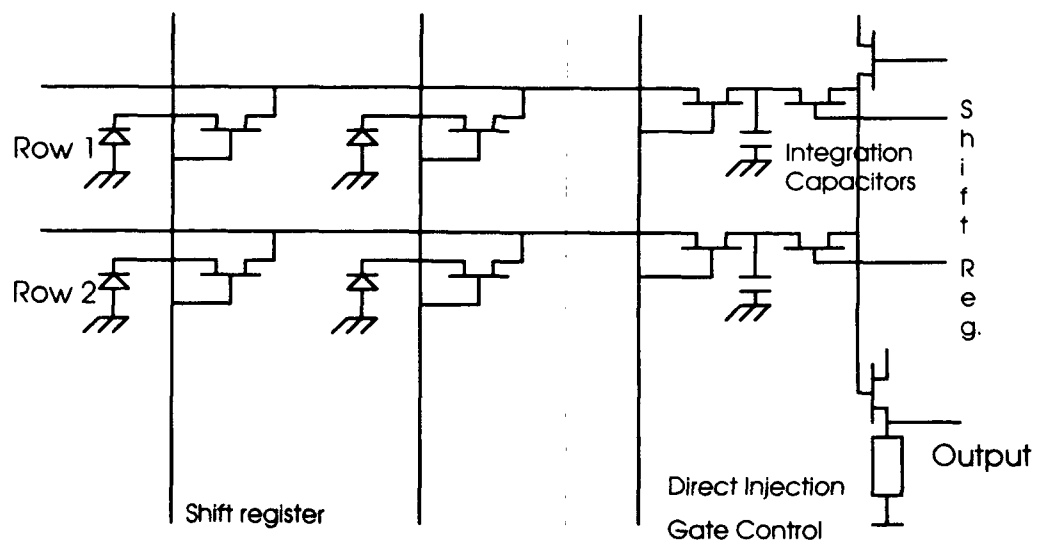$$\sigma_s^2 = \frac{Ta^2}{2\pi} \tag{9}$$

If the noise signal is a current with power spectral density of amps^{2}Hz^{-1} the integrated signal is a charge (in coulombs) and the variance of the integrated signal has the units of coulombs^2.

THIS IS A BLANK PAGE
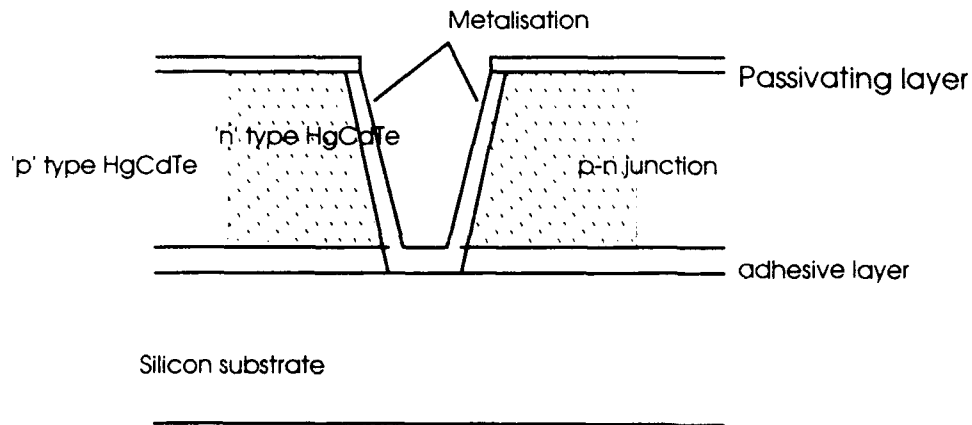
Figure 1: Construction of a photodiode using the 'loophole' technique

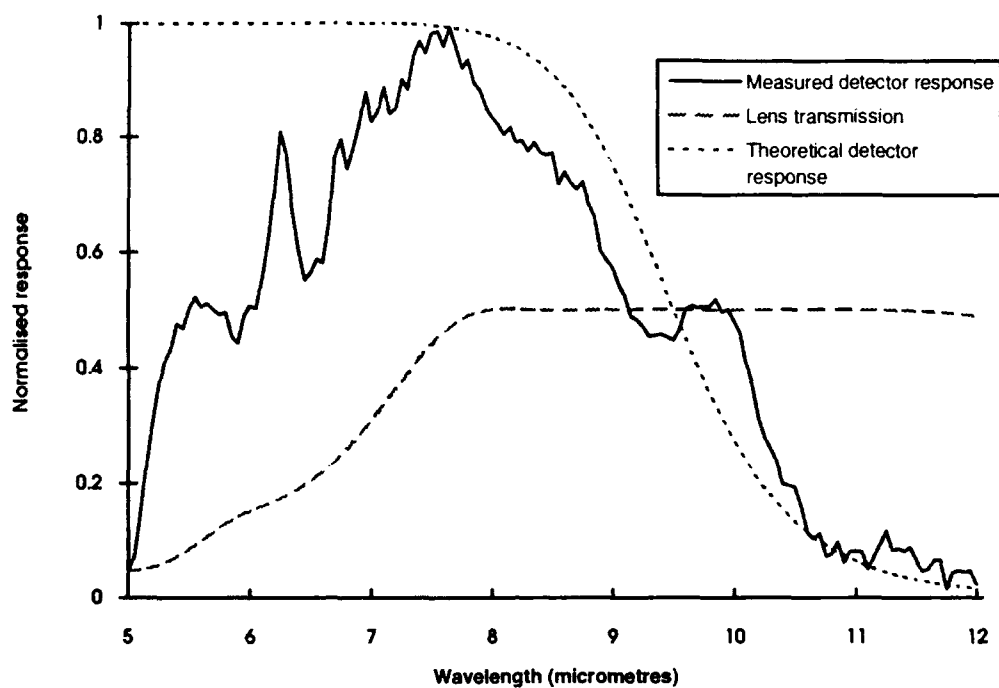**Figure 2: Simplified schematic of MESA detector array architecture**

Figure 3: Variation of measured lens transmission, detector spectral response and theoretical detector spectral response with wavelength
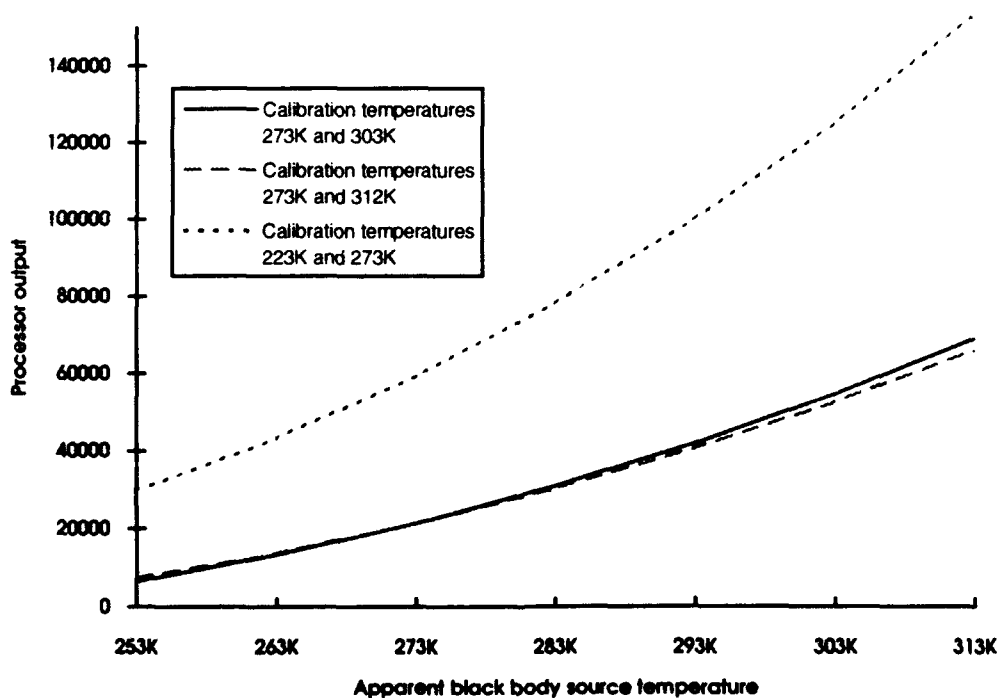

Figure 4: Variation of responsivity nonuniformity compensation processor output with apparent black body source temperature
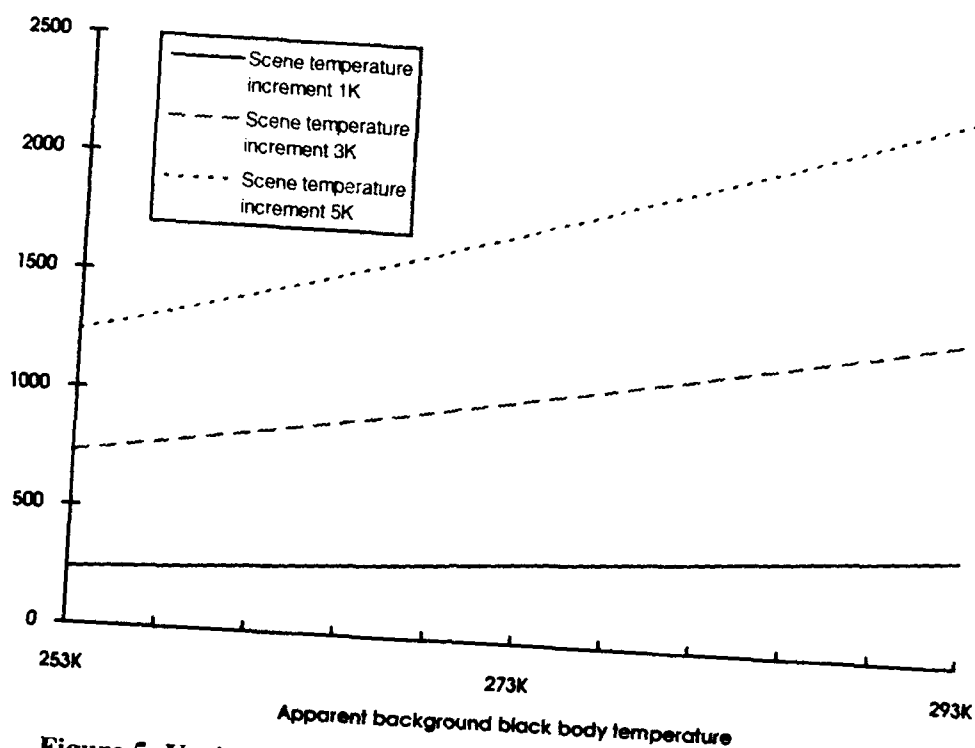
Figure 5: Variation of scene data with apparent source to background temperature difference and background temperature
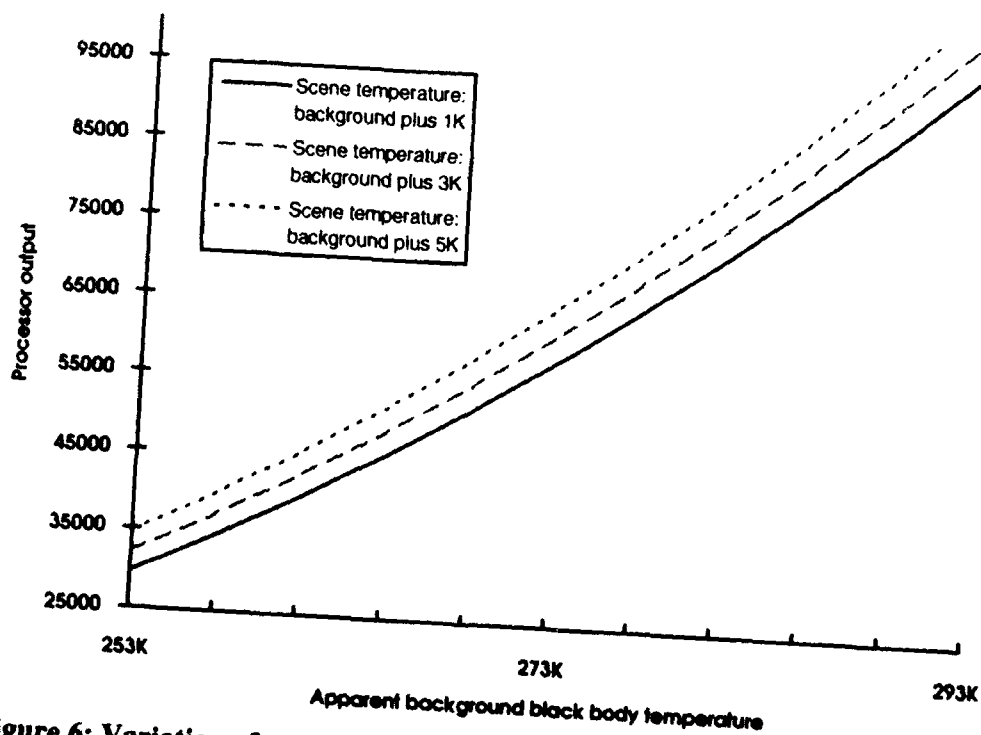

Figure 6: Variation of processor output with apparent background temperature for calibration source temperatures of 223 K and 273 K.

THIS IS A BLANK PAGE

DISTRIBUTION

	Copies
Defence Science and Technology Organisation	
Chief Defence Scientist	)
Central Office Executive	) 1 shared copy
Counsellor, Defence Science, London	Cont Sht
Counsellor, Defence Science, Washington	Cont Sht
Scientific Adviser POLCOM	1
Senior Defence Scientific Adviser	1
Navy Office	
Navy Scientific Adviser	1
Air Office	
Air Force Scientific Adviser	1
Army Office	
Scientific Adviser, Army	1
Defence Intelligence Organisation	
Scientific Adviser, Defence Intelligence Organisation	1
Surveillance Research Laboratory	
Director	1
Chief, Optoelectronics Division	1
Research Leader, Optoelectronics Systems	1
Head, Systems Analysis	1
Head, Image Processing	1
Optoelectronics Division HQ	2
Mr G.V. Poropat (Author)	2
Electronics Research Laboratory	
Research Leader, Seeker Technology, GWD	1
Head, Advanced Seekers, GWD	1
Head, Optoelectronic Warfare, EWD	1
Mr R. Oerman	1
Media Services	1
Libraries and Information Services	
Australian Government Publishing Service	1
Defence Central Library, Technical Reports Centre	1
Manager, Document Exchange Centre, (for retention)	1
National Technical Information Service, United States	2
Defence Research Information Centre, United Kingdom	2
Director Scientific Information Services, Canada	1
Ministry of Defence, New Zealand	1
National Library of Australia	1

	Copies
Defence Science and Technology Organisation Salisbury, Research Library	2
Library Defence Signals Directorate, Melbourne	1
British Library Document Supply Centre	1

Spares

Defence Science and Technology Organisation Salisbury, Research Library	6

Total 41

Department of Defence	Page Classification UNCLASSIFIED
DOCUMENT CONTROL DATA SHEET	Privacy Marking/Caveat (of Document)

1a. AR Number AR-008-154	1b. Establishment Number SRL-0114-RN	2. Document Date August 1993	3. Task Number ADA 87/026	

4. Title TESTING AND CHARACTERISATION OF THE 'CYCLOPS' HgCdTe FOCAL PLANE DETECTOR ARRAY	5. Security Classification $\boxed{U}$ $\boxed{U}$ $\boxed{U}$ Document Title Abstract S (Secret) C (Confi) R (Rest) ∪ (Unclass) * For UNCLASSIFIED docs with a secondary distribution LIMITATION, use (L) in document box.	6. No. of Pages 26
		7. No. of Refs 15

8. Author(s) G.V. Poropat	9. Downgrading/Delimiting Instructions N/A

10a. Corporate Author and Address Surveillance Research Laboratory PO Box 1500 SALISBURY SA 5108	11. Officer/Position responsible for Security.................................SOSRL................... Downgrading.............................DSRL......................
10b. Task Sponsor DGFD (AIR)	Approval for Release........DSRL...............................

12. Secondary Distribution of this Document

    Approved for Public Release

Any enquiries outside stated limitations should be referred through DSTIC, Defence Information Services, Department of Defence, Anzac Park West, Canberra, ACT 2600.

13a. Deliberate Announcement

    No limitation

13b. Casual Announcement (for citation in other documents)	$\boxed{\checkmark}$ No Limitation
	$\boxed{}$ Ref. by Author , Doc No. and date only.

14. DEFTEST Descriptors Focal plane arrays, Infrared detectors, Performance evaluation	15. DISCAT Subject Codes 170501

16. Abstract

Optoelectronics Division has developed an advanced technology demonstrator utilising an infrared focal plane detector array to assess the feasibility of using passive infrared sensors for ADF applications. To model the performance of the sensor the characteristics of the focal plane detector array have been measured. The measurement of the characteristics of large scale detector arrays and the testing of these arrays present problems which are not encountered with single element infrared detectors. Optoelectronics Division has gained considerable experience in these processes during the development of the 'Cyclops' technology demonstrator. The procedures used in characterising the HgCdTe focal plane detector array and the results obtained are described.

Doc Sect WF11

16. Abstract (CONT.)

17. Imprint

Surveillance Research Laboratory
PO Box 1500
SALISBURY SA 5108

18. Document Series and Number	19. Cost Code	20. Type of Report and Period Covered
SRL-0114-RN		RESEARCH NOTE

21. Computer Programs Used

N/A

22. Establishment File Reference(s)

N/A

23. Additional information (if required)